Digestive Diseases and Sciences (2018) 63:3398–3408
https://doi.org/10.1007/s10620-018-5268-0

ORIGINAL ARTICLE

Silybin Alleviates Hepatic Steatosis and Fibrosis in NASH Mice by Inhibiting Oxidative Stress and Involvement with the Nf-κB Pathway

Qiang Ou[1] · Yuanyuan Weng[2] · Siwei Wang[2] · Yajuan Zhao[1] · Feng Zhang[2] · Jianhua Zhou[1,3] · Xiaolin Wu[1,3]

Received: 27 February 2018 / Accepted: 28 August 2018 / Published online: 6 September 2018
© Springer Science+Business Media, LLC, part of Springer Nature 2018

Abstract

Background and Aim Silybin is the major biologically active compound of silymarin, the standardized extract of the milk thistle (*Silybum marianum*). Increasing numbers of studies have shown that silybin can improve nonalcoholic steatohepatitis (NASH) in animal models and patients; however, the mechanisms underlying silybin's actions remain unclear.

Methods Male C57BL/6 mice were fed a methionine-choline deficient (MCD) diet for 8 weeks to induce the NASH model, and silybin was orally administered to the NASH mice. The effects of silybin on lipid accumulation, hepatic fibrosis, oxidative stress, inflammation-related gene expression and nuclear factor kappa B (NF-κB) activities were evaluated by biochemical analysis, immunohistochemistry, immunofluorescence, quantitative real-time PCR and western blot.

Results Silybin treatment significantly alleviated hepatic steatosis, fibrosis and inflammation in MCD-induced NASH mice. Moreover, silybin inhibited HSC activation and hepatic apoptosis and prevented the formation of MDBs in the NASH liver. Additionally, silybin partly reversed the abnormal expression of lipid metabolism-related genes in NASH. Further study showed that the nuclear factor erythroid 2-related factor 2 (Nrf2) signaling pathway played important roles in the silybin-derived antioxidant effect, as evidenced by the upregulation of Nrf2 target genes in the silybin treatment group. In addition, silybin significantly downregulated the expression of inflammation-related genes and suppressed the activity of NF-κB signaling.

Conclusions Silybin was effective in preventing the MCD-induced increases in hepatic steatosis, fibrosis and inflammation. The effect was related to alteration of lipid metabolism-related gene expression, activation of the Nrf2 pathway and inhibition of the NF-κB signaling pathway in the NASH liver.

Keywords Silybin · Nonalcoholic steatohepatitis · Oxidative stress · NF-κB signaling pathway

Qiang Ou and Yuanyuan Weng have contributed equally to this work.

✉ Feng Zhang
felix.f.zhang@outlook.com

✉ Jianhua Zhou
shprozhou@163.com

✉ Xiaolin Wu
wuxiaolin999@hotmail.com

Qiang Ou
ouqiang76@163.com

Yuanyuan Weng
605742738@qq.com

Siwei Wang
358031289@qq.com

Yajuan Zhao
zhaoyajuan1970@163.com

[1] The Eighth People's Hospital of Shanghai, No. 8 Caobao Road, Shanghai 200235, China

[2] Department of Clinical Laboratory, Core Facility, Quzhou People's Hospital, Quzhou, Zhejiang 324000, China

[3] The Central Laboratory of the Eighth People's Hospital of Shanghai, No. 8 Caobao Road, Shanghai 201508, China

Introduction

Nonalcoholic fatty liver disease (NAFLD) is the most common type of chronic liver disease in both developed and developing countries [1]. NAFLD ranges in severity from steatosis to nonalcoholic steatohepatitis (NASH), which can lead to liver fibrosis, cirrhosis and ultimately hepatocellular cancer [2]. It is estimated that the prevalence of NAFLD is approximately 25% worldwide. In China, the prevalence of NAFLD is greater than 15% [3]. Currently, NASH, as a pivotal early stage of NAFLD, is the third most common indication for liver transplantation in the USA and has been predicted to become the first one between 2020 and 2025 [4]. The etiology of NASH remains elusive. The "two hit theory" is generally accepted. The first hit is insulin resistance (IR), causing accumulation of lipids in the hepatocytes. This increases the sensitivity of the liver to the second hit, which may be oxidative stress, lipid peroxidation and proinflammatory cytokines, leading to the initiation and progression of NASH [5]. Therefore, blocking oxidative stress and/or inflammatory responses is critical in preventing the progression of NASH [6]. Since effective therapies for NASH remain limited, searching for a safe and effective drug is important.

Silybin (Fig. 1) is the major biologically active compound of silymarin, the standardized extract of the milk thistle (*Silybum marianum*) [7]. Silybin has multiple pharmacological effects, such as anti-lipid peroxidation, anti-hepatic fibrosis and anti-inflammation effects [8, 9]. It is widely used in the treatment of various liver diseases because of its hepatoprotective effects [8–10]. Increasing numbers of studies have indicated that silybin treatment improves hyperlipidemia and hepatic fibrosis and inhibits inflammation in patients or animal models with NASH [11–14]. However, the molecular mechanisms associated with the hepatoprotective activity of silybin in NASH remain to be elucidated. In this study, we evaluated the efficacy of silybin in protecting the liver against MCD-induced NASH in mice and investigated the underlying mechanisms of its action. Our study demonstrated that silybin improved MCD-induced liver injury by regulating lipid metabolism-related genes, abating oxidative stress and suppressing inflammation.

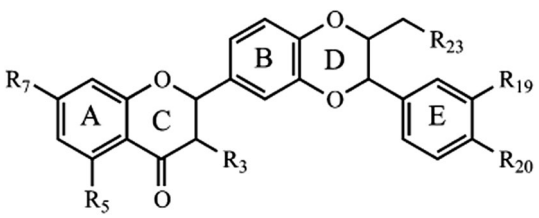

Fig. 1 General structure of silybin

Materials and Methods

Animals and Experimental Design

Healthy 6-week-old male C57BL/6 mice were purchased from the Shanghai Xi Puer-Bikai Experimental Animal Co., Ltd (Shanghai, China). All mice were housed in cages under standard conditions with free access to food and water. Animals were randomly divided into three groups and treated as follows: (1) control group ($n=6$); (2) NASH group ($n=6$); and (3) silybin-treated NASH model group ($n=6$). Mice in the NASH group were fed an MCD diet. Mice in the control group were fed the same diet, but it was sufficient in DL-methionine (3 g/kg) and choline bitartrate (2 g/kg). NASH mice were dosed with silybin orally, at a dose of 105 mg/kg/day. At the end of 8 weeks of diet administration and treatment, the mice were anesthetized after 12 h of fasting and killed. Blood samples were collected from the femoral aorta, and serum was isolated for biochemical analyses. Livers were removed and weighed. Liver tissue was rapidly dissected. Partial liver samples were snap-frozen in liquid nitrogen and stored at − 80 °C for biochemical and gene expression analysis. A small piece of the liver sample was fixed in 4% paraformaldehyde for further histological analysis.

These animal studies were approved by the Animal Ethics Committee of the Eighth People's Hospital of Shanghai. All the surgical and experimental procedures were in accordance with institutional animal care guidelines.

Detection of Serum and Liver Biochemistry

Serum triglycerides (TG), total cholesterol (TC) and the activities of the liver-associated enzymes alanine aminotransferase (ALT) and aspartate aminotransferase (AST) were estimated with an automatic biochemical analyzer (Roche P800 Modular). Hepatic homogenates were used for the determination of glutathione peroxidase (GPX), superoxide dismutase (SOD) and TG and TC content using a kit (Nanjing Jianchen Institute of Bioengineering, China). For determination of TG and TC contents, tissue lipids were extracted with methanol/chloroform (1:2).

Morphological Examinations

The liver sample removed from each mouse was fixed in 4% paraformaldehyde for 96 h. After dehydrating it in graded alcohol and embedding it in paraffin wax, sections were cut to a thickness of 4 μm. Liver pathology was assessed by HE, and picrosirius red staining was used to

assess collagen fibers in the liver tissues. Each section was assessed under 10 × 20 light microscopic fields.

Real-Time Polymerase Chain Reaction Analysis of Liver RNA

Total liver RNA was isolated using TRIzol Reagent (Invitrogen, USA). Real-time polymerase chain reaction (RT-PCR) analysis was performed with QuantiTecTM SYBR Green PCR (Qiagen, German) according to the manufacturer's instructions. The sequences of the primers are listed in Table 1. The expression levels of the target mRNA were measured using an ABI 7500 PCR machine (ABI, USA). Each sample was run and analyzed in duplicate. Target mRNA levels were adjusted to the values relative to GAPDH, which was used as the endogenous control. The fold changes relative to control values were obtained and used to express the experimental change in gene expression.

Immunofluorescence and Immunohistochemistry

Liver tissues were fixed overnight in a 4% formaldehyde solution. Sections were prepared according to the standard procedure. Paraffin-embedded sections were deparaffinized with xylene, dehydrated in decreasing concentrations of ethanol, then processed in 10 mM citrate buffer (pH 6.0), and heated in a microwave oven for 15 min for antigen retrieval. The tissue sections were permeabilized by 0.2% Triton-X 100 for 10 min. For immunohistochemistry staining, liver sections were treated with 3% hydrogen peroxidase for 10 min to block endogenous peroxidase activity and incubated with blocking buffer containing 5% (w/v) bovine serum albumin (BSA). Then, the sections were incubated with the primary antibodies, followed by incubation with the biotinylated secondary antibodies. The following primary antibodies were used: anti-cytochrome P450 2E1 (CYP2E1; BA4717, Boster Bioengineering Co. Ltd., Wuhan, China), anti-α-SMA (ab5694, Abcam) and anti-4 hydroxynonenal (4-HNE; ab46545, Abcam). For immunofluorescence assays, the following primary and secondary antibodies were used: anti-ubiquitin (ab7780, Abcam), anti-F4/80 (ab6640, Abcam), anti-CD68 (ab955, Abcam), Alexa Fluor-488-labeled goat anti-rabbit (A-11008; Thermo Fisher Scientific) and chicken anti-rat IgG (A-21470; Thermo Fisher Scientific). The stained area was quantified in six randomly selected 200 × microscopic fields per mouse section using ImageJ software (ImageJ2x).

TUNEL Assay

Apoptotic cell death in the liver sections was examined by using a TUNEL Apoptosis Detection Kit (Alexa Fluor 488, QcBio Science & Technologies Co., Ltd, Shanghai, China)

Table 1 Primer sequence of RT-PCR

Target gene	Sequence (5′–3′)
Srebf1	
F	TCTTTCCTGGCTTGTCCTTTGGGA
R	AGGTGGCTCAACATAGCATCACCA
Fas	
F	CTGCGGAAACTTCAGGAAATG
R	GGTTCGGAATGCTATCCAGG
Accα	
F	AGGAGGACCGCATTTATCGAC
R	TGACCGTGGGCACAAAGTT
Pparγ	
F	AGGGCGATCTTGACAGGAAAGACA
R	ATCTCTTGCACGGCTTCTACGGAT
Pparα	
F	AAACAAGTGCCAGCCAGGTTTGAC
R	ACAGAACAGCTCAAATTGCCACCG
Cpt1A	
F	TGGCATCATCACTGGTGTGTT
R	GTCTAGGGTCCGATTGATCTTTG
Acox1	
F	CTTGTTCGCGCAAGTGAGG
R	CAGGATCCGACTGTTTAC C
Mttp	
F	TCTCACAGTACCCGTTCTT
R	TCTTCTCCGAGAGACATATCC
ApoB	
F	TTGGCAAACTGCATAGCATCC
R	TCAAATTGGGACTCTCCTTTAGC
Gclm	
F	ACAGGTAAAACCAAATAGTAACCAAGTTAA
R	TGTTTAGCAAATGCAGTCAAATCTG
Gclc	
F	GATGCTGTCTTGCAGGGAATG
R	AGCGAGCTCCGTGCTGTT
Nqo1	
F	CAGCAGACGCCCCAATTC
R	TGGTGTCTCATCCCAAATATTCTC
Hmox1	
F	CCTCACTGGCAGGAAATCATC
R	CCTCGTGGAGACGCTTTACATA
Gstm1	
F	AGTCCACACAGCCTTCATTC
R	CAGGCTGGCACTCAAGTATT
IL-6	
F	TCCTACCCCAACTTCCAATGCTC
R	TTGGATGGTCTTGGTCCTTAGCC
IL-1β	
F	TTCAGGCAGGCAGTATCACTC
R	GAAGGTCCACGGGAAAGACAC
IL-12β	
F	CTGGAGCACTCCCCATTCCTA

Table 1 (continued)

Target gene	Sequence (5′–3′)
R	GCAGACATTCCCGCCTTTG
TNF-α	
F	GACGTGGAACTGGCAGAAGAG
R	ACCGCCTGGAGTTCTGGAA
CCL2	
F	TTAAAAACCTGGATCGGAACCAA
R	GCATTAGCTTCAGATTTACGGGT
CXCL10	
F	CCAAGTGCTGCCGTCATTTTC
R	TCCCTATGGCCCTCATTCTCA
Gapdh	
F	GCCAGCCTCGTCTCATAGACA
R	AGAGAAGGCAGCCCTGGTAAC

F forward primer, *R* reverse primer

as described in the manufacturer's instructions. The number of TUNEL positive cells was assessed in six randomly selected 200 × microscopic fields per mouse using ImageJ software (ImageJ2x).

Western Blot Analysis

Frozen tissues were homogenized in 1 × SDS lysis buffer containing protease inhibitor cocktail (Roche) and phosphatase inhibitor cocktail (1 mM sodium orthovanadate, 5 mM sodium fluoride, 3 mM β-glycerophosphate and 4 mM sodium tartrate) by a homogenizer and a sonicator on ice. The samples were centrifuged at 13,400 rpm at 4 °C for 20 min, and the supernatants were collected. Equal amounts of protein were separated on 8% SDS-PAGE and transferred to a PVDF membrane (Millipore, MA). After blocking for 1 h at room temperature in Tris-buffered saline containing 0.1% Tween-20 and 0.5% casein, the membrane was probed with the primary antibody overnight at 4 °C, followed by incubation with HRP-conjugated secondary antibodies for an hour at room temperature. Immune complexes were detected by the Tanon 4200SF system from Tanon Biotechnology (Shanghai, China). Band intensity was quantified using ImageJ software (ImageJ2x). The primary antibodies used in this study were anti-p-IKKα/β (#2697), anti-IKKβ (#2370), anti-p-IκBα (#2859), anti-IκBα (#4812), anti-p-p65 (#3033), anti-p65 (#4764, Cell Signaling Technology, Danvers, MA) and anti-β-actin (#A1978, Sigma, St. Louis, MO).

Statistical Analysis

All data are expressed as the mean ± standard deviation (SD). The principal statistical test was the *t*-test (two-tailed with unequal variance). $P < 0.05$ was considered statistically significant. Statistical analysis was performed using SPSS 19.0.0 software (SPSS, Inc., Chicago, IL, USA).

Results

Effects of Silybin on MCD Diet-Induced NASH Mice

After eating an MCD diet for 8 weeks, the NASH mouse model was successfully established, as reflected by distinctive changes in both serum and liver tissue. The MCD diet resulted in significant weight loss in mice. Treatment with silybin significantly attenuated weight loss (Fig. 2a, $p < 0.05$). Serum ALT and AST activities were obviously higher, while TG and TC were significantly decreased, in the NASH group compared with the controls. Treatment of NASH mice with silybin resulted in a significant reduction in serum ALT and AST levels but had no effect on serum TC and TG levels (Fig. 2b, c, $p < 0.05$ or $p < 0.01$). Hepatic TG content was higher in the MCD diet-induced mice compared with the control mice. However, this accumulation was attenuated by silybin supplementation. Hepatic TC content did not show any difference between groups (Fig. 2c, $p < 0.01$). The results of HE staining (Fig. 2d) showed that the liver tissue from the control group had distinct hepatic lobule, central vein and portal areas, without inflammatory cell infiltrations or hepatic fatty droplets. However, the liver of NASH mice displayed disordered hepatic lobules, pronounced hepatic steatosis and hepatocellular ballooning with inflammatory cell infiltrations. All these changes were relieved by treatment with silybin. Overall, the NAFLD activity score was significantly increased in the NASH group but decreased in the silybin-treated mice (Fig. 2e, $p < 0.01$).

Effects of Silybin on Hepatic Fibrosis and Hepatic Stellate Cell Activation

As shown in Fig. 3, the NASH liver displayed marked collagen fiber proliferation after picrosirius red staining, while a lower level of collagen fiber staining was observed in the control and silybin treatment mice. The expression of α-SMA, a reliable marker of hepatic stellate cell (HSC) activation that precedes fibrous tissue deposition [15], was higher in the NASH group than in the control group and was significantly reduced by silybin treatment (Fig. 3). These results were quantified, and the data further confirmed that silybin can reduce liver fibrosis ($p < 0.05$ or $p < 0.01$).

Effects of Silybin on Hepatic Apoptosis and Ubiquitin

It has been reported that hepatocyte apoptosis triggers HSC activation and liver fibrosis [16, 17]. MCD diet feeding

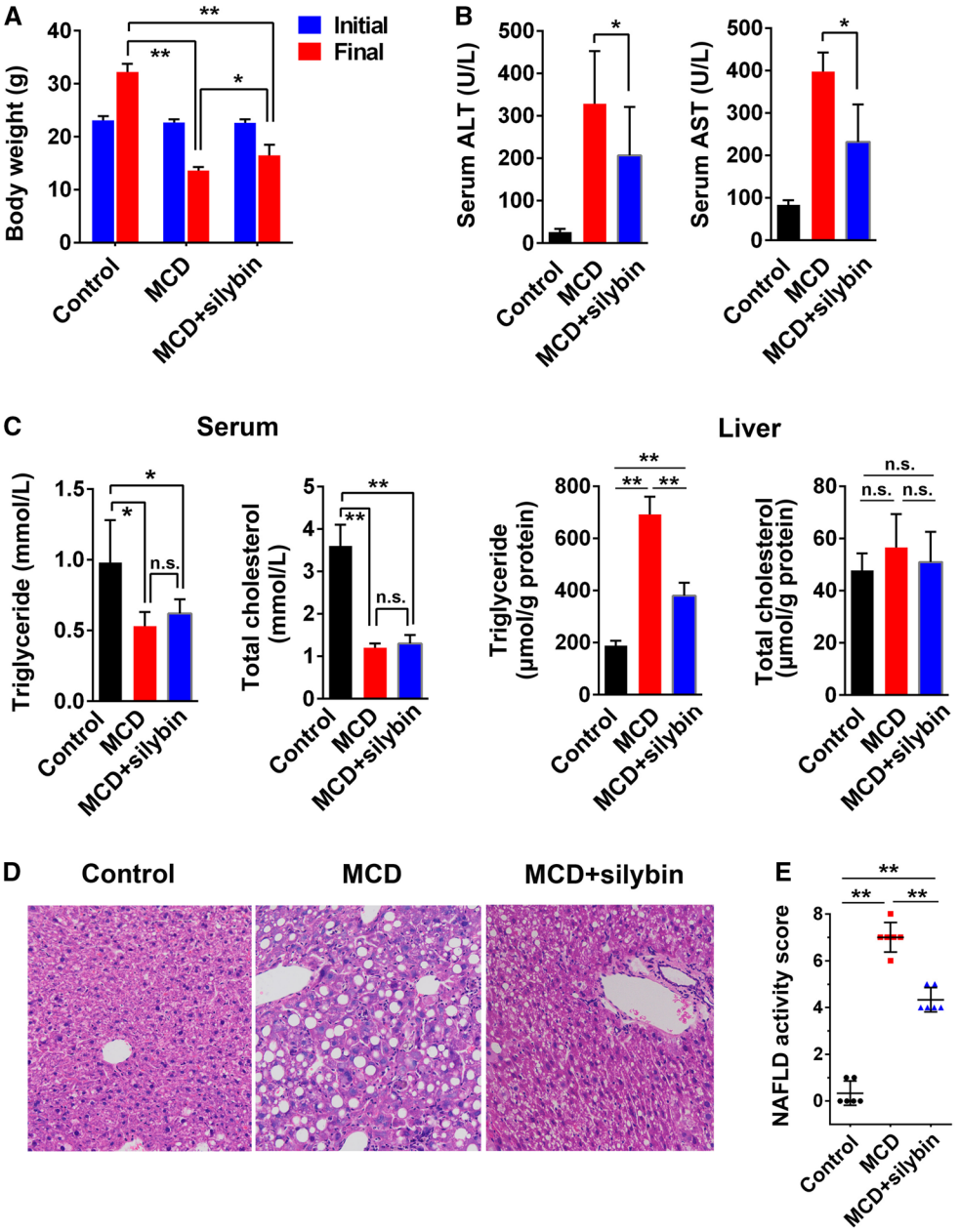

Fig. 2 The effect of silybin on the MCD-fed mice. **a** The body weights in different groups. **b**, **c** Serum biochemical parameters and hepatic TG and TC contents in the different groups. **d** Representative microscopic photographs of liver sections stained with HE (original magnification, ×200). E: NAFLD activity scores in different groups. Data are expressed as the mean ± SD ($n = 6$ in each group). *$p < 0.05$; **$p < 0.01$

increased the number of apoptotic cell deaths detected by TUNEL staining (Fig. 4a). Ubiquitin, as a marker of Mallory-Denk bodies (MDBs), indicates hepatocellular damage in NASH [18, 19]. An increase in the level of ubiquitin staining of cells was also observed in the NASH liver (Fig. 4b). It is noteworthy that treatment with silybin reduced these changes (Fig. 4a, b). These results suggest that silybin had hepatoprotection effects.

Effects of Silybin on Lipid Metabolism-Related Gene Expression

The MCD diet did not change hepatic *Fas*, but tended to decrease hepatic *Srebf1* mRNA levels and increased *Accα* and *Pparγ* mRNA levels. Although silybin had no effect on *Fas* and *Srebf1* mRNA levels in the NASH liver, it reversed the changes in *Accα* and *Pparγ* mRNA levels (Fig. 5a). The

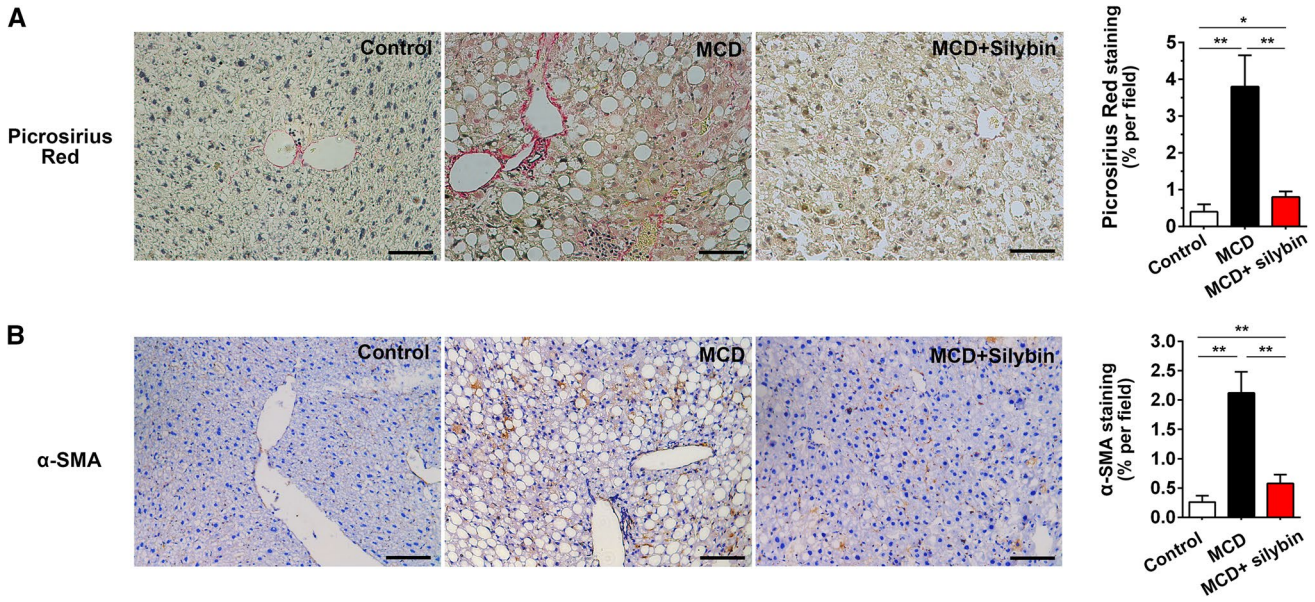

Fig. 3 The effects of silybin on hepatic fibrosis and hepatic stellate cell activation. **a** Representative microscopic photographs of liver sections stained with picrosirius red (original magnification, ×200) and quantitative analysis of changes in different groups. **b** The expression level of hepatic α-SMA was determined by immunohistochemistry staining. Right, quantitative analysis of the α-SMA positive area in different groups. Data are expressed as the mean ± SD ($n = 6$ in each group). *$p < 0.05$; **$p < 0.01$

MCD diet reduced the hepatic *Pparα* and *Acox1* mRNA levels, which were significantly increased by silybin treatment. The levels of *Cpt1A* were not changed by the MCD diet but were significantly augmented by silybin (Fig. 5b). In contrast, the MCD diet had no effect on the hepatic *ApoB* mRNA levels, which were also not changed by silybin, whereas the MCD diet attenuated *Mttp* mRNA levels, which were increased by silybin (Fig. 5c).

Effects of Silybin on MCD Diet-Induced Oxidative Stress in the Liver

Hepatic induction of CYP2E1 is a major pathway involved in oxidative stress [20]. CYP2E1 activation leads to the generation of reactive oxygen species (ROS), causing lipid oxidation (LPO) products to be generated [21]. To evaluate the role of silybin in oxidative stress, CYP2E1 and 4-HNE (one of the major LPO products) were detected. As shown in Fig. 6a, b, the expression levels of CYP2E1 and 4-HNE were significantly increased in the livers of NASH mice compared with the control mice. However, silybin significantly decreased the expression of CYP2E1 and 4-HNE in the livers of the NASH mice. These results were confirmed by semi-quantitative analysis of the CYP2E1 and 4-HNE positive areas.

Previous studies have shown that the activation of nuclear factor erythroid 2-related factor 2 (Nrf2) signaling is essential for hepatic cytoprotection against oxidative stress [22]. To explore whether the alleviation of oxidative stress by silybin was related to the activation of the Nrf2 pathway, the Nrf2-dependent antioxidant genes were detected, including γ-glutamylcysteine synthetase modifier subunit (*GCLM*), catalytic subunit (GCLC), NAD(P)H quinone oxidoreductase 1 (*NQO1*), heme oxygenase-1 (*HMOX1*) and glutathione S-transferase Mu 1 (*GSTM1*). The results showed that the MCD diet only affected the expression levels of *GCLC* and *NQO1*. (*GCLC* was slightly lower, and *NQO1* was elevated.) It is noteworthy that all of the Nrf2-dependent antioxidant genes detected in this study were significantly upregulated by silybin (Fig. 6c, $p < 0.05$ or $p < 0.01$). The hepatic contents of GPX and SOD, two anti-oxidative enzymes, were lower in NASH mice than in control mice, while silybin treatment fully normalized GPX and SOD activities (Fig. 6d, $p < 0.01$). These results suggest that the anti-oxidative effects of silybin are involved in regulating multiple anti-oxidative gene levels.

Effects of Silybin on Hepatic Inflammation-Related Gene Expression

As shown in Fig. 7a, compared with the control group, the mRNA levels of *IL-6*, *IL-1β*, *IL-12β*, *TNF-α*, *CCL2* and *CXCL10* were upregulated in the MCD-induced NASH group ($p < 0.05$ or $p < 0.01$). Silybin significantly inhibited the MCD-induced elevation of the expression levels of these genes. Accordingly, the protein levels of p-IKKα/β, p-IkBα and p-p65 were increased in the NASH liver, which were then significantly decreased by silybin. IkBα expression

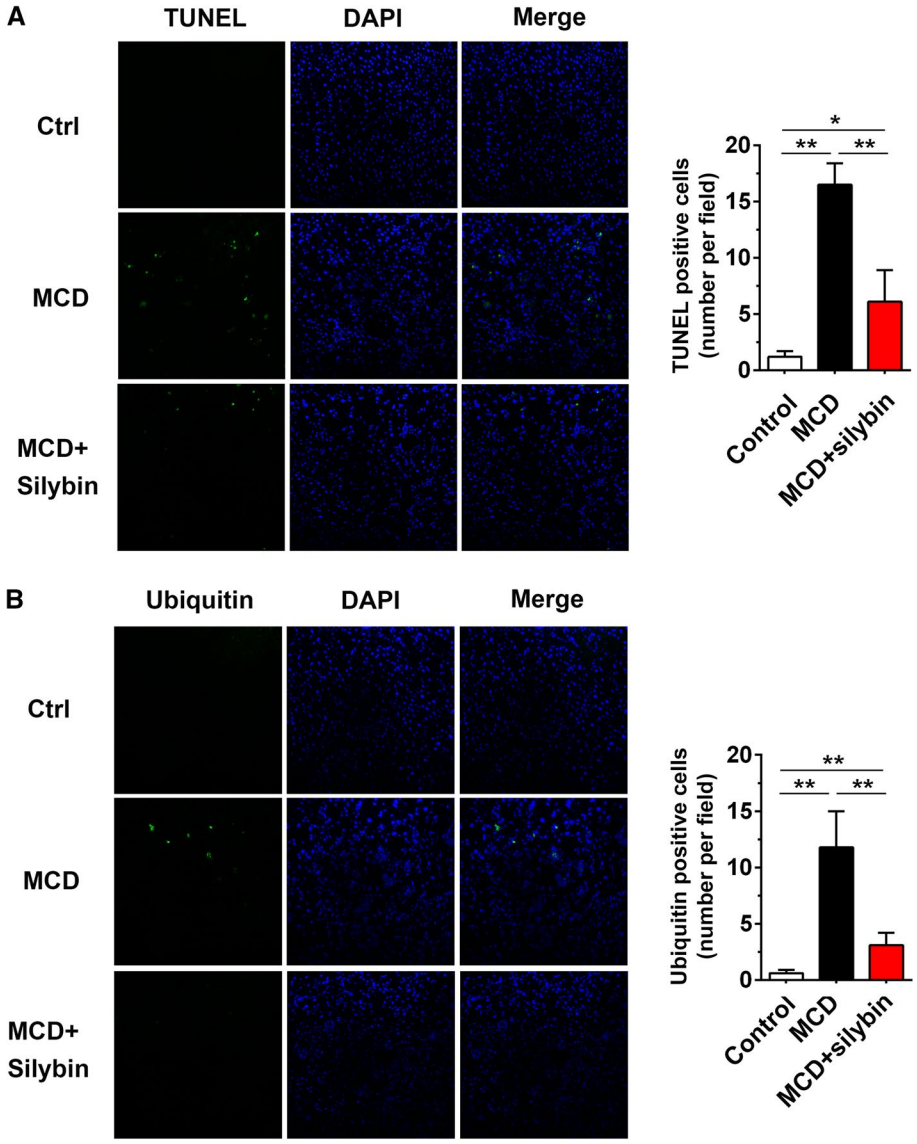

Fig. 4 Effect of silybin on hepatic apoptosis and ubiquitin. **a** Representative images (magnification, × 200) of TUNEL and quantitative analysis of TUNEL positive cells in different groups. **b** The expression of ubiquitin was detected by immunofluorescence and quantitative analysis of ubiquitin positive cells in different groups. Data are expressed as the mean ± SD ($n = 6$ in each group). *$p < 0.05$; **$p < 0.01$

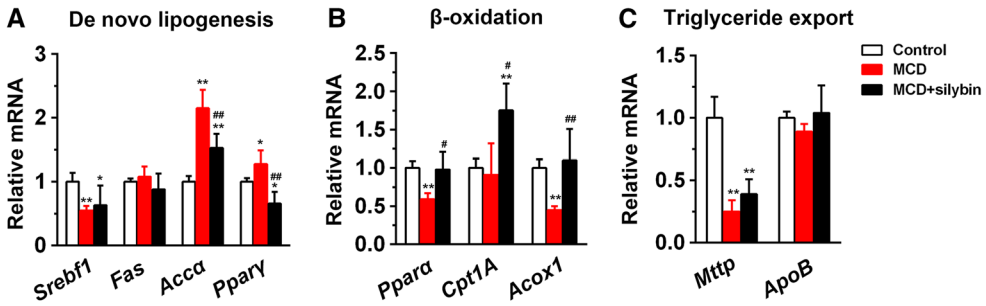

Fig. 5 Effect of silybin on lipid metabolism-related gene expression. The relative mRNA expressions of de novo lipogenesis-related genes (**a**), β-oxidation-related genes (**b**) and triglyceride export genes (**c**) were evaluated. The results represent three independent experiments, and data are expressed as the mean ± SD ($n = 3$ in each group). *$p < 0.05$; **$p < 0.01$ compared to the control group; $^{\#}p < 0.05$; $^{\#\#}p < 0.01$ compared to the MCD group

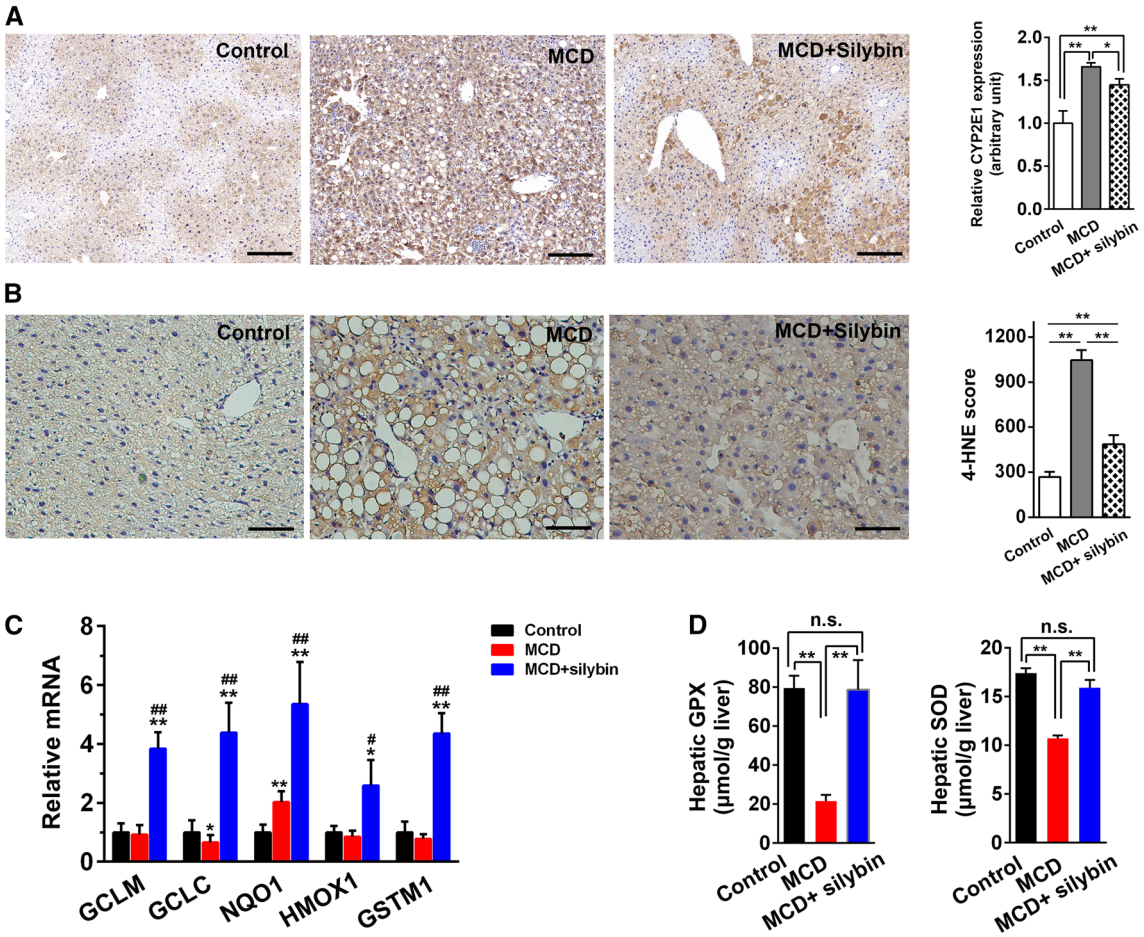

Fig. 6 Silybin reduces MCD diet-induced oxidative stress. The CYP2E1 expression (**a**) and 4-HNE expression (**b**) in different groups. **c** Expression of Nfr2 target genes was detected by qRT-PCR analysis. The results represent three independent experiments. **d** The levels of GPX and SOD in hepatic tissue in the different groups. Data are expressed as the mean ± SD ($n = 6$ in each group). $^{*}p < 0.05$; $^{**}p < 0.01$ compared to the control group; $^{\#}p < 0.05$; $^{\#\#}p < 0.01$ compared to the MCD group

was reduced in the NASH liver, and this change was also reversed by silybin treatment. These results were further confirmed by assessing the relative protein expression of these genes (Fig. 7b). To assess the role of silybin in liver inflammation, the number of macrophages was detected using F4/80 and CD68 immunofluorescence staining. As shown in Fig. 7c, compared to the control group, the proportions of F4/80 and CD68 positive cells were increased in NASH liver and decreased after silybin treatment.

Discussion

It has been previously observed that silybin could improve NASH in animal models and NAFLD patients; however, the exact mechanisms remain unclear [11, 12, 14, 23]. In this study, we demonstrated that the hepatoprotective effect of silybin on the MCD diet-induced NASH mouse model was dependent on its antioxidant stress and anti-inflammatory activities.

Several diet-based animal models with NASH have been established, such as the high-fat diet, the high-cholesterol and high-fat diet, and the MCD diet. The MCD diet is efficient and reproducible for inducing severe liver damage and progressive fibrosis in mice [24]. The MCD diet-induced NASH model is considered convenient for studying the role of oxidant stress and inflammation in NASH development [25, 26]. We established an NASH mouse model by feeding them an MCD diet for 8 weeks, as confirmed by biochemical and histologic findings, which are consistent with the previous reports on this model [27]. These biochemical and histologic parameters were considerably improved by silybin treatment (Figs. 2, 3). These results demonstrated that silybin improved liver function and alleviated hepatic steatosis and fibrosis, suggesting the therapeutic effects of silybin in MCD diet-induced NASH.

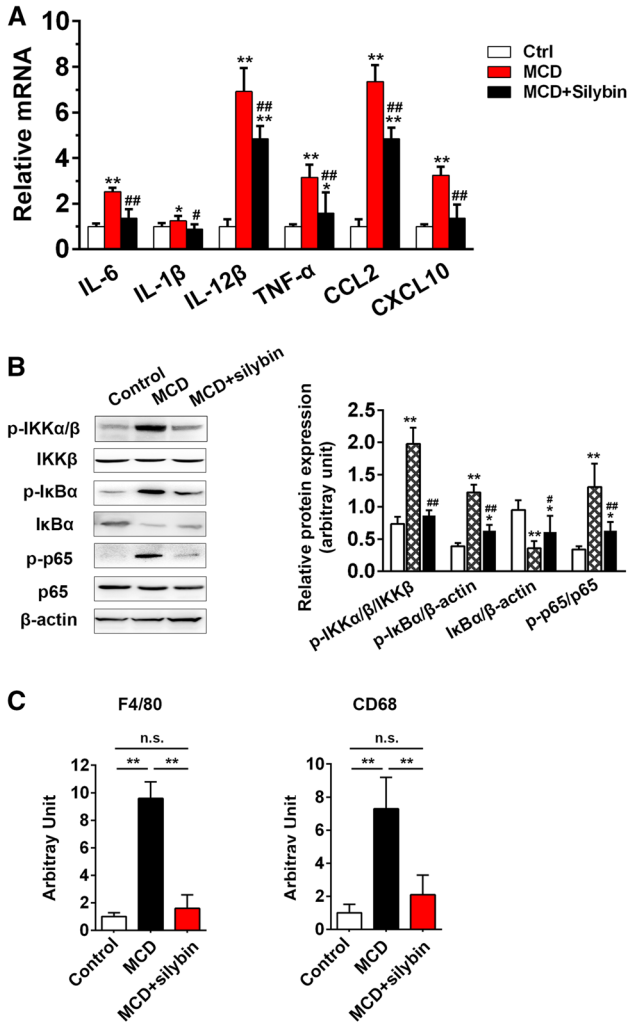

Fig. 7 Effect of silybin on MCD diet-induced hepatic inflammation. **a** The relative mRNA expression of pro-inflammatory cytokines and chemokines in livers from different treatments. The results represent three independent experiments. **b** The activation of NF-κB signaling in livers of the different groups was evaluated by western blot. Quantification of protein expression was in the right panel ($n=3$). **c** Immunofluorescence staining was performed with anti-F4/80 and CD68 antibodies to determine the number of macrophages. The results are expressed as the proportion of positive cells (compared with the control group), and data are expressed as the mean ± SD ($n=4$ in each group). $^{*}p<0.05$; $^{**}p<0.01$ compared to the control group; $^{\#}p<0.05$; $^{\#\#}p<0.01$ compared to the MCD group

HSCs switching from quiescent to fibrogenic active stellate cells are the key target in the progression of NASH [28]. In our study, the level of α-SMA in the liver of NASH mice was downregulated by treatment with silybin (Fig. 3). In line with this result, hepatocyte apoptosis, as an important factor inducing HSC activation, was also decreased by silybin (Fig. 4a). These results suggested that the role of silybin in preventing hepatic fibrosis may involve inhibiting HSC activation. MDBs are found in various hepatic diseases, including NAFLD [19, 29]. MDB formation indicates the severity of hepatocyte balloon degeneration and often occurs in NASH [19], and silybin prevented increased MDB formation in the NASH liver in our study. These results indicate that silybin has hepatoprotection effects.

Although serum TC and TG were not affected, markedly alleviated steatohepatitis and ameliorated liver function were observed after silybin treatment (Fig. 2), which correlated with downregulation of the expression of the adipogenic genes Accα and Pparγ in the NASH liver (Fig. 5). These results are consistent with that reported by Peizhen Xiao et al. who proved that silymarin decreases the expression of the adipogenic genes in grass carp [30]. However, silybin showed no obvious effect on the levels of *Fas* and their upstream gene *Srebf1*. *Srebf1* is an important lipogenic enzyme gene. It encodes the protein SREBP-1 in human, which has been proven to be increased in high-fat diet-induced NASH, while it is decreased in MCD-induced NASH [24, 31]. In this study, the decreased *Srebf1* level in NASH liver was not obviously changed by silybin.

With regard to the expression of hepatic β-oxidation-related genes, silybin administration enhanced the mRNA level of *Cpt1A* and reversed the MCD-induced decrease in *Pparα* and *Acox1* mRNA levels. These results suggest that silybin stimulated hepatic lipid oxidation in this NASH model. For genes involved in triglyceride export, *Mttp* is an important regulator of hepatic lipid excretion in hepatocytes. Silybin slightly increased the mRNA levels of *Mttp*, which were reduced by the MCD diet, indicating that silybin was involved in modification of hepatic FFA excretion.

Oxidative stress is considered to be the critical phenomenon in the progression from fatty liver to steatohepatitis. CYP2E1 is one of the isoenzymes of cytochrome P450 and plays a key role in promoting oxidative stress, causing LPO products to be generated [20, 21]. Studies have shown that CYP2E1 is increased in the livers of NAFLD patients [32, 33], and CYP2E1 knockout prevented progression of alcohol- or high-fat diet-induced steatohepatitis [34]. Silybin showed anti-oxidative effects in this study because the increased tissue levels of CYP2E1 and 4-HNE in the model group were restored by silybin treatment (Fig. 6a). Accordingly, the Nrf2-dependent antioxidant genes, including *GCLM*, *GCLC*, *NQO1*, *HMOX1* and *GSTM1,* were also significantly upregulated by silybin treatment, further indicating that silybin may act as a novel Nrf2 inducer (Fig. 6b). These results raise the possibility of novel roles of silybin in oxidative stress. In addition, two major intracellular antioxidant enzymes, hepatic GPX and SOD, which were decreased in the MCD-induced NASH group, were recovered significantly by silybin treatment (Fig. 6c). These results are consistent with the previous reports that silybin treatment significantly increased the activities of SOD and GPX in alcohol-induced fatty liver [35, 36]. Therefore, silybin protects liver against MCD diet-induced oxidative stress

by regulating multiple key molecules in the process of oxidative stress.

Inflammation is considered to be another important mediator in the progression of NASH [1]. The inhibitory effect of silybin on NF-κB signaling during liver injury has been reported by several studies [36, 37]. Few reports have focused on whether the hepatoprotective effects of silybin on MCD-induced NASH were related to inhibition of NF-κB activation. Our data showed that silybin significantly reduced the level of p-IKKα/β and its downstream effector factors, p-IkBα and p-p65 (Fig. 7b). Accordingly, the enhanced transcription of several major pro-inflammatory cytokines in NASH, such as TNF-α, IL-6, IL-1β and IL-12β, were attenuated by silybin supplementation (Fig. 7a). These results were in line with the well-established anti-inflammation function of silybin.

Two chemokines, *CCL2* and *CXCL10,* have been proven to be important in the induction of important pro-inflammatory cytokines and the activation of the NF-κB pathway [38, 39]. The enhanced expressions of *CCL2* and *CXCL10* and the increased proportion of F4/80 and CD68 positive cells, which reflect the recruitment of macrophages in NASH, were also decreased due to the actions of silybin (Fig. 7a, c). These results further confirmed that silybin possesses an anti-inflammatory effect in MCD-induced NASH.

In the present study, we observed that silybin attenuated hepatic steatosis and fibrosis in MCD diet-induced NASH mice. Its mechanisms may be related to alleviating MCD-induced oxidative stress and inflammation, probably by regulating lipid metabolism-related gene expression, upregulating Nfr2 target genes, reducing pro-inflammatory cytokine production and inhibiting the activation of the NF-κB pathway. Our study confirms the therapeutic effect of silybin on MCD diet-induced NASH. These results have encouraged us to develop further investigations to better understand its exact molecular mechanisms.

Acknowledgments This work was supported by the National Natural Science Foundation of China (81670129 to Xiaolin Wu).

Compliance with ethical standards

Conflict of interest There is no conflict of interest to disclose.

References

1. Harmon RC, Tiniakos DG, Argo CK. Inflammation in non-alcoholic steatohepatitis. *Expert Rev Gastroenterol Hepatol*. 2011;5:189–200.
2. Bellentani S, Marino M. Epidemiology and natural history of non-alcoholic fatty liver disease (NAFLD). *Ann Hepatol*. 2009;8:S4–S8.
3. Fan JG, Farrell GC. Epidemiology of non-alcoholic fatty liver disease in China. *J Hepatol*. 2009;50:204–210.
4. Wree A, Broderick L, Canbay A, Hoffman HM, Feldstein AE. From NAFLD to NASH to cirrhosis-new insights into disease mechanisms. *Nat Rev Gastroenterol Hepatol*. 2013;10:627–636.
5. Day CP, James OF. Steatohepatitis: a tale of two "hits"? *Gastroenterology*. 1998;114:842–845.
6. Takaki A, Kawai D, Yamamoto K. Multiple hits, including oxidative stress, as pathogenesis and treatment target in non-alcoholic steatohepatitis (NASH). *Int J Mol Sci*. 2013;14:20704–20728.
7. Abenavoli L, Capasso R, Milic N, Capasso F. Milk thistle in liver diseases: past, present, future. *Phytother Res*. 2010;24:1423–1432.
8. Aghazadeh S, Amini R, Yazdanparast R, Ghaffari SH. Anti-apoptotic and anti-inflammatory effects of Silybum marianum in treatment of experimental steatohepatitis. *Exp Toxicol Pathol*. 2011;63:569–574.
9. Cacciapuoti F, Scognamiglio A, Palumbo R, Forte R, Cacciapuoti F. Silymarin in non alcoholic fatty liver disease. *World J Hepatol*. 2013;5:109–113.
10. Marino Z, Crespo G, D'Amato M, et al. Intravenous silibinin monotherapy shows significant antiviral activity in HCV-infected patients in the peri-transplantation period. *J Hepatol*. 2013;58:415–420.
11. Hajiaghamohammadi AA, Ziaee A, Oveisi S, Masroor H. Effects of metformin, pioglitazone, and silymarin treatment on Nonalcoholic Fatty liver disease: a randomized controlled pilot study. *Hepat Mon*. 2012;12:e6099.
12. Yao J, Zhi M, Gao X, Hu P, Li C, Yang X. Effect and the probable mechanisms of silibinin in regulating insulin resistance in the liver of rats with Nonalcoholic fatty liver. *Braz J Med Biol Res*. 2013;46:270–277.
13. Solhi H, Ghahremani R, Kazemifar AM, Hoseini Yazdi Z. Silymarin in treatment of Nonalcoholic steatohepatitis: A randomized clinical trial. *Caspian J Intern Med*. 2014;5:9–12.
14. Wah Kheong C, Nik Mustapha NR, Mahadeva S. A randomized trial of silymarin for the treatment of nonalcoholic steatohepatitis. *Clin Gastroenterol Hepatol*. 2017;15:1940–1949. **e1948**.
15. Carpino G, Morini S, Ginanni Corradini S, et al. Alpha-SMA expression in hepatic stellate cells and quantitative analysis of hepatic fibrosis in cirrhosis and in recurrent chronic hepatitis after liver transplantation. *Dig Liver Dis*. 2005;37:349–356.
16. Eguchi A, De Mollerat Du, Jeu X, Johnson CD, Nektaria A, Feldstein AE. Liver Bid suppression for treatment of fibrosis associated with NonalcoholicNonalcoholic steatohepatitis. *J Hepatol*. 2016;64:699–707.
17. Guicciardi ME, Gores GJ. Apoptosis as a mechanism for liver disease progression. *Semin Liver Dis*. 2010;30:402–410.
18. Banner BF, Savas L, Zivny J, Tortorelli K, Bonkovsky HL. Ubiquitin as a marker of cell injury in nonalcoholic steatohepatitis. *Am J Clin Pathol*. 2000;114:860–866.
19. Kayacetin S, Basaranoglu M. Mallory-Denk bodies: correlation with steatosis, severity, zonal distribution, and identification with ubiquitin. *Turk J Gastroenterol*. 2015;26:506–510.
20. Abdelmegeed MA, Banerjee A, Yoo SH, Jang S, Gonzalez FJ, Song BJ. Critical role of cytochrome P450 2E1 (CYP2E1) in the development of high fat-induced Nonalcoholic steatohepatitis. *J Hepatol*. 2012;57:860–866.
21. Teufel U, Peccerella T, Engelmann G, et al. Detection of carcinogenic etheno-DNA adducts in children and adolescents with Nonalcoholic steatohepatitis (NASH). *Hepatobiliary Surg Nutr*. 2015;4:426–435.
22. Lee LY, Kohler UA, Zhang L, et al. Activation of the Nrf2-ARE pathway in hepatocytes protects against steatosis in nutritionally induced Nonalcoholic steatohepatitis in mice. *Toxicol Sci*. 2014;142:361–374.
23. Marin V, Gazzin S, Gambaro SE, et al. Effects of oral administration of silymarin in a juvenile murine model of Nonalcoholic steatohepatitis. *Nutrients* 2017;9.

24. Rinella ME, Elias MS, Smolak RR, Fu T, Borensztajn J, Green RM. Mechanisms of hepatic steatosis in mice fed a lipogenic methionine choline-deficient diet. *J Lipid Res*. 2008;49:1068–1076.
25. Marcolin E, Forgiarini LF, Tieppo J, Dias AS, Freitas LA, Marroni NP. Methionine- and choline-deficient diet induces hepatic changes characteristic of Nonalcoholic steatohepatitis. *Arq Gastroenterol*. 2011;48:72–79.
26. Phung N, Pera N, Farrell G, Leclercq I, Hou JY, George J. Pro-oxidant-mediated hepatic fibrosis and effects of antioxidant intervention in murine dietary steatohepatitis. *Int J Mol Med*. 2009;24:171–180.
27. Schattenberg JM, Galle PR. Animal models of Nonalcoholic steatohepatitis: of mice and man. *Dig Dis*. 2010;28:247–254.
28. Higashi T, Friedman SL, Hoshida Y. Hepatic stellate cells as key target in liver fibrosis. *Adv Drug Deliv Rev*. 2017;121:27–42.
29. Liu H, Gong M, French BA, Li J, Tillman B, French SW. Mallory-Denk Body (MDB) formation modulates Ufmylation expression epigenetically in alcoholic hepatitis (AH) and Nonalcoholic steatohepatitis (NASH). *Exp Mol Pathol*. 2014;97:477–483.
30. Xiao P, Yang Z, Sun J, et al. Silymarin inhibits adipogenesis in the adipocytes in grass carp Ctenopharyngodon idellus in vitro and in vivo. *Fish Physiol Biochem*. 2017;43:1487–1500.
31. Jha P, Knopf A, Koefeler H, et al. Role of adipose tissue in methionine-choline-deficient model of Nonalcoholic steatohepatitis (NASH). *Biochim Biophys Acta*. 2014;1842:959–970.
32. Aubert J, Begriche K, Knockaert L, Robin MA, Fromenty B. Increased expression of cytochrome P450 2E1 in nonalcoholic fatty liver disease: mechanisms and pathophysiological role. *Clin Res Hepatol Gastroenterol*. 2011;35:630–637.
33. Weltman MD, Farrell GC, Hall P, Ingelman-Sundberg M, Liddle C. Hepatic cytochrome P450 2E1 is increased in patients with nonalcoholic steatohepatitis. *Hepatology*. 1998;27:128–133.
34. Maher J. The CYP2E1 knockout delivers another punch: first ASH, now NASH. Alcoholic steatohepatitis Nonalcoholic steatohepatitis. *Hepatology*. 2001;33:311–312.
35. Das SK, Mukherjee S. Biochemical and immunological basis of silymarin effect, a milk thistle (Silybum marianum) against ethanol-induced oxidative damage. *Toxicol Mech Methods*. 2012;22:409–413.
36. Zhang W, Hong R, Tian T. Silymarin's protective effects and possible mechanisms on alcoholic fatty liver for rats. *Biomol Ther (Seoul)*. 2013;21:264–269.
37. Vecchione G, Grasselli E, Voci A, et al. Silybin counteracts lipid excess and oxidative stress in cultured steatotic hepatic cells. *World J Gastroenterol*. 2016;22:6016–6026.
38. Zhang X, Shen J, Man K, et al. CXCL10 plays a key role as an inflammatory mediator and a non-invasive biomarker of Nonalcoholic steatohepatitis. *J Hepatol*. 2014;61:1365–1375.
39. Marra F, Tacke F. Roles for chemokines in liver disease. *Gastroenterology*. 2014;147:577–594. **e571**.